01 Nov 2004

Liquid Holdup and Pressure Drop in the Gas-Liquid Cocurrent Downflow Packed-Bed Reactor under Elevated Pressures

Jing Guo

Muthanna H. Al-Dahhan
Missouri University of Science and Technology, aldahhanm@mst.edu

Recommended Citation

J. Guo and M. H. Al-Dahhan, "Liquid Holdup and Pressure Drop in the Gas-Liquid Cocurrent Downflow Packed-Bed Reactor under Elevated Pressures," *Chemical Engineering Science*, vol. 59, no. 22 thru 23, pp. 5387 - 5393, Elsevier, Nov 2004.
The definitive version is available at https://doi.org/10.1016/j.ces.2004.07.106

ELSEVIER

Chemical Engineering Science 59 (2004) 5387–5393

Chemical Engineering Science

www.elsevier.com/locate/ces

Liquid holdup and pressure drop in the gas–liquid cocurrent downflow packed-bed reactor under elevated pressures

Jing Guo, Muthanna Al-Dahhan*

Department of Chemical Engineering, Chemical Reaction Engineering Laboratory (CREL),Washington University, Campus Box 1198, One Brooking Dr., St. Louis, MO 63130, USA

Received 28 February 2004; received in revised form 26 June 2004; accepted 12 July 2004
Available online 30 September 2004

Abstract

An experimental investigation of the residence time distribution, liquid holdup, and pressure drop in a gas–liquid downflow packed bed reactor with porous particles operated under elevated pressures is presented. The effects of the two-phase flow rates and reactor pressures on the external liquid holdup and pressure drop are discussed. A mechanistic model, which accounts for the interaction between the gas and liquid phases by incorporating the shear and velocity slip factors between phases, is employed to predict the external liquid holdup and pressure drop for the experimentally covered flow regime. The involved parameters, such as shear and velocity slip factors and Ergun single-phase flow bed constants, are calculated from the correlations developed via neural network regression. The model's predictions and the experimental observations at elevated pressure are compared.

Keywords: Packed bed; Multiphase flow; Moment analysis; Porous media; Pressure drop; Residence time distribution

1. Introduction

Trickle-bed reactors (TBR) with gas–liquid cocurrent downflow are employed in three-phase processes that require a relatively large liquid residence time to achieve the necessary degree of reactant conversion. In particular, the development of efficient and economically feasible processes for wastewater treatment at intermediate levels of organic waste concentration is of considerable industrial interest. It has been reported that the continuous processes in a three-phase reactor in a trickle bed regime are suitable in mild conditions for the catalytic treatment of aqueous solutions with pollutant loading (Fortuny et al., 1995).

Air oxidation of aqueous organic waste over Al–Fe pillared clay catalysts has been studied in our previous work with a continuous stirred basket reactor. To apply such reaction kinetics in the trickle bed reactor, one has to learn the corresponding liquid phase residence time distribution for each experimental measurement of the reactant conversion at the reactor outlet. The residence time is determined by the liquid holdup, which is closely interlinked with reaction conversion and selectivity, interfacial mass transfer, and power consumption (Iliuta et al., 1998). As a fundamental parameter to characterize the flow resistance inside the reactor, two-phase pressure drop is also a focus of the hydrodynamics studies in the literature (Al-Dahhan and Dudukovic, 1994; Al-Dahhan et al., 1997). Most of the literature studies on quantifying liquid holdup and pressure drop have been carried out under atmospheric pressure. The operation of catalytic wet oxidation, however, is usually carried out at elevated pressure (1–5 MPa) in order to increase the solubility of the gaseous reactants in the liquid phase. Due to the lack of reliable experimental data under elevated-pressure operation over porous catalyst, our understanding of hydrodynamics under these operating conditions is still unclear.

Due to the complex interaction between the flowing fluids and the stationary porous packing, few fundamental

* Corresponding author. Tel.: +1-314-935-7187; fax: +1-314-935-7211.
E-mail address: muthanna@che.wustl.edu (M. Al-Dahhan).

0009-2509/$ - see front matter © 2004 Elsevier Ltd. All rights reserved.
doi:10.1016/j.ces.2004.07.106

approaches are available to depict the hydrodynamic phenomena. A phenomenological model based on a simple physical picture of the phenomena involved is preferred to empirical correlations. So far, several phenomenological models have been proposed and widely adopted in the literature, such as the slit based model of Holub et al. (1992) and its extended version for high pressure and high gas flow rates modified by Al-Dahhan et al. (1998) and Iliuta et al. (1998).

Therefore, the present work focuses on the experimental investigation of the residence time distribution, liquid holdup, and pressure drop over porous Al–Fe pillared clay catalyst particles in a TBR, which is operated under the similar operating conditions used for the reaction of CWO of aqueous phenol solution. To evaluate the capability of the extended slit based model, comparisons between experimental observations and the predictions of liquid holdup and pressure drop are presented.

2. Experimental work

The experiments were carried out at room temperature and elevated pressure (0.8–2.2 MPa), with water as the liquid phase and air as the gas phase. Hydrodynamics were investigated for superficial liquid flow rates from 2 to 9.2 ml/ min (0.08–0.37 $kg/m^2/s$) and for superficial gas mass flux between 0.03 and 0.26 $kg/m^2/s$ (superficial gas velocity between 0.10 and 2.82 cm/s). The reactor was made of a $\varnothing 2.1\times$ 30 cm stainless steel tubing. The extruded Al–Fe pillared clay catalyst particles, in cylindrical form ($\varnothing 2.0 \times 8.0$ mm, approximately) and with particle porosity 0.42, were supported by a stainless steel screen placed near the bottom of the reactor tube. The value of pore volume was given as 0.33 cm^3/g. Two packing procedures were taken. The catalysts were loaded portion by portion with either long duration severe vibrating or recursively gentle tapping, resulting in the bed porosities of 0.43, and 0.55, respectively.

The liquid holdup were deduced from residence time distribution measurement via tracer technique after the reactor system is brought to steady state at the desired conditions. The local concentrations of the tracer were simultaneously measured through the electrical conductivity of the water at the inlet and outlet of the packed-bed. The conductivity of the water is measured using a conductivity meter (YSI Model 35) and recorded as a function of time using a computer-based data acquisition system. The National Instruments LabVIEW program was used to record, plot, and process the tracer response data. Through experimentation, a pulse injection of 0.02 mg/ml KCl solution was found to give the best response. The pressure drop measurements were taken with a pressure transducer connected to two pressure taps located at the bottom and the top of the packed-bed. Pressure drop along the reactor was measured using a Validyne model CD-223 pressure transducer with the diaphragm sensor of model DP15-24.

Before the experiments are started the reactor is flooded with liquid phase for 10 h followed by draining so that packing gets prewetted. Then high liquid flow rates are chosen for the high interaction between gas and liquid, followed by reducing the liquid flow rate to the desired level. Such procedure helps minimizing liquid–gas maldistribution and hysteresis (Levec et al., 1986).

3. Results and discussion

Fig. 1 shows typical evolution of the packed bed operation from unstable to stable status. After a time, the mean value of the filtered data of the pressure drop became constant, which indicated stable reactor status. The raw pressure drop data captured by the pressure transducer were filtered in a standard low-pass Butterworth filter to reduce the noise of the curve. Due to the presence of the bubbles, the conductivity data obtained via the conductance meter were filtered using the algorithm that combines the standard Butterworth with an iterative methodology to remove the biased noise added by the bubble passages (Gupta et al., 1999).

The segment between the tracer inlet and outlet points is comprised of distributors, a packed bed section of the catalyst used, and pipe connections. However, only the packed bed section is of real interest. The residence of tracer in the distributor and the pipes, called the “inactive zone” in this work, caused significant artifacts in the final response curve captured by the outlet conductance meter. Hence, for each operating condition, we also tested the tracer response curve for the inactive zone by removing the packing section and passing the tracer through the inactive zone only.

In a bed with porous particles, both interphase and intraparticle phenomena affect the residence time distribution measurements. Comparison of the response E curves at the inlet and outlet with respect to time shows that the liquid flow behavior is deviated from plug flow because of the long

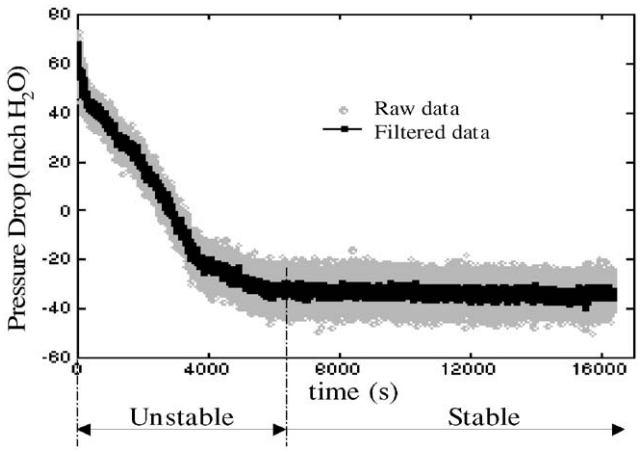

Fig. 1. Signal evolution of pressure drop of two-phase downflow in packed-bed. Liquid flow rate: 4 ml/min, gas superficial velocity: 1.44 cm/s, reactor pressure: 0.8 MPa, bed porosity: 0.55.

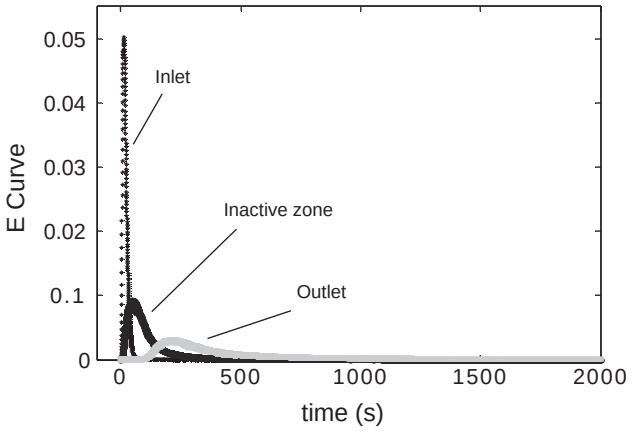

Fig. 2. Typical filtered curve of tracer response measured at inlet, outlet and for inactive zone. Liquid flow rate: 8 ml/min, gas superficial velocity: 1.44 cm/s, reactor pressure: 0.8 MPa, bed porosity: 0.55.

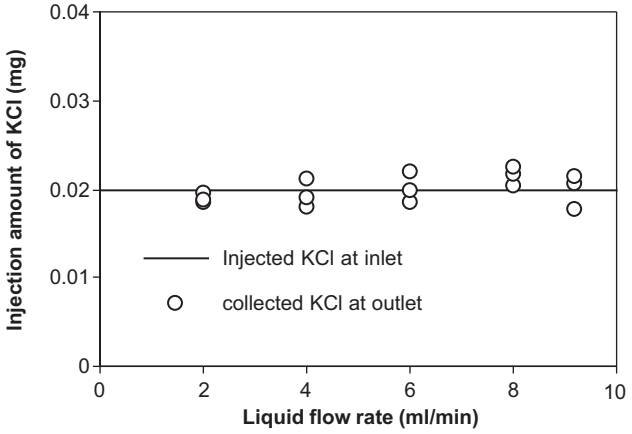

Fig. 3. Tracer mass balance over the porous catalyst. Bed porosity: 0.43, reactor pressure: 0.8 MPa.

tails in the outlet response curve, as shown in Fig. 2. It is clear that the tracer residence time in the inactive zone is significant, and the time delay and measurement errors due to the inactive zone were not negligible compared to the time scale for the packing section. Tracer diffusion is assumed to be the mechanism acting to create the long tails of the residence time distribution curve. For a porous particle, when the concentration gradient is favorable for inward diffusion, tracer is transferred from the liquid bulk to the liquid contained in the solid pores through a mass transfer film around the particle. Inside the pore, tracer diffuses toward the core of the particle. Iliuta et al. (1996) studied the tracer accessibility into porous particles and found that the accessibility of the catalyst pores decreases with increasing liquid flow rate due to the decrease of the contact time of the liquid with the solid particles. To test the possibility of the adsorption of the tracer onto the catalyst pore, the tracer mass balance for both the reactor input and output responses were checked, as shown in Fig. 3. It turns out that the tracer adsorption was reversible from the catalyst pore because the mass balance of the tracer was still conserved. When the gradient of tracer concentration is favorable for outward diffusion, the tracer diffuses back from the core of the particle to the liquid bulk.

Once the tracer response curve was obtained, the first moment was calculated to determine the residence time and the liquid holdup. According to Sater and Levenspiel (1966), the first and second moments of the bed between two probes can be obtained from the difference in first and second moments (variance) seen by the probes

$$\mu_i = \frac{\int_0^\infty t C_i \,\mathrm{d}t}{\int_0^\infty C_i \,\mathrm{d}t} = \int_0^\infty t E(t)\,\mathrm{d}t,$$
$$\sigma_i^2 = \frac{\int_0^\infty t^2 C_i \,\mathrm{d}t}{\int_0^\infty C_i \,\mathrm{d}t} - \mu_i^2 = \int_0^\infty t^2 E(t)\,\mathrm{d}t - \mu_i^2, \quad (1)$$

where the subscript $i = 0$, 1, 2 stands for the inlet position, the end of inactive zone, and the outlet position, respectively. The residence time and the dimensionless second moment of tracer through the packed bed section are obtained by Eq. (2):

$$\tau = \mu_2 - \mu_1, \quad \sigma_{\theta,r}^2 = \frac{\sigma_r^2}{\tau^2} = \frac{\sigma_{\theta,2}^2 - \sigma_{\theta,1}^2}{\tau^2}. \quad (2)$$

The residence time of catalyst bed is related to the total liquid holdup ($\varepsilon_{l,t}$) via Eq. (3)

$$\varepsilon_{l,t} = \frac{u_L * \tau}{L_r}, \quad (3)$$

where u_L is the superficial liquid phase flow rate. The total holdup of the liquid phase in the packed bed is generally expressed as a fractional bed volume, i.e., as the volume of liquid present per volume of empty reactor. It consists of two parts, the external holdup (ε_e) partially occupying the void volume of the packed bed and the internal holdup (ε_i) held inside the pores of the catalyst by capillary forces. The internal volume of the catalyst particle is assumed to be totally wetted, which is reasonable since the catalyst has been prewetted by the flooded flow for 10 h before the start of experiments. The relationship between the different portions of the liquid holdup can be established using the following formulas, where ε_B is the bed porosity, and ε_p is the particle porosity.

$$\varepsilon_e = \varepsilon_{l,t} - \varepsilon_i, \quad \varepsilon_i = (1 - \varepsilon_B)\varepsilon_p. \quad (4)$$

The external liquid holdup is a key parameter for the design of packed beds, which consists of dynamic and static holdup. It is related to other important hydrodynamic issues, such as the external wetting of the catalyst and the pressure gradient, which in turn affect the reaction selectivity depending on the level of liquid spreading on the catalyst surface. The liquid holdup results from the balance between the driving forces and the resistances. As shown in Fig. 4a, the external liquid holdup for a porous particle decreases in

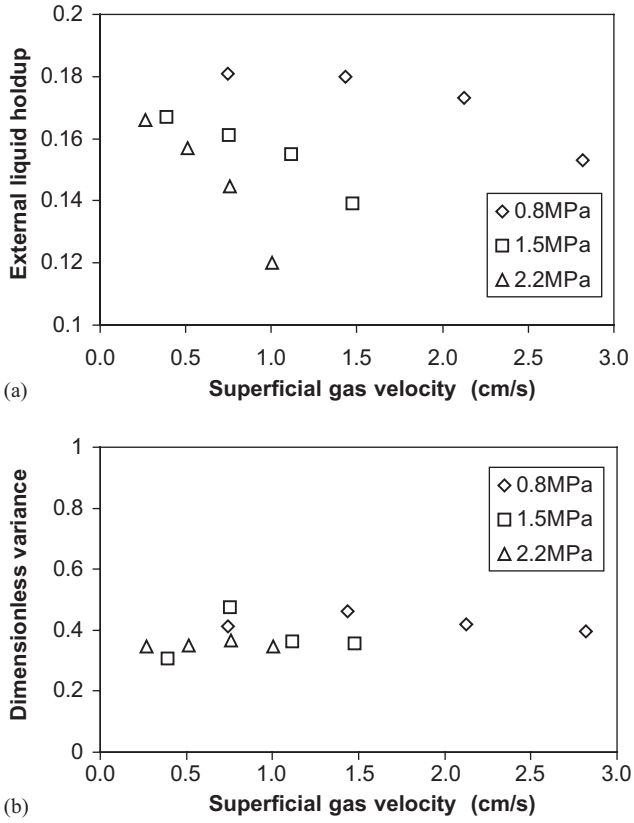

Fig. 4. Effect of pressure on (a) liquid holdup and (b) dimensionless variance of tracer curve. Liquid flow rate: 9.2 ml/min (mass flux: 0.37 $kg/m^2/s$), bed porosity: 0.43.

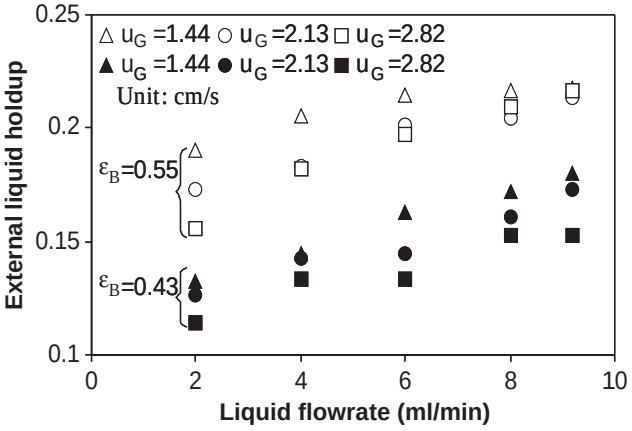

Fig. 5. Effects of liquid and gas flow rate on liquid holdup, reactor pressure: 0.8 MPa. (note: 10 ml/min leads to liquid mass flux 0.4 $kg/m^2/s$).

two-phase operation with an increase in the superficial gas velocity at fixed pressure. This effect becomes more prominent at higher reactor pressure. Apparently the gas flow significantly influences the gas–liquid interaction at elevated pressures in the trickle flow regime, as reported by Al-Dahhan et al. (1997). To account for the effect of the gas pressure and gas flow rate on the external liquid holdup, the relative contribution of the different components of the driving force has to be taken into consideration. These components consist of gravitational force, gas–liquid interfacial drag force, and the pressure gradient due to the distribution of the local pressure field. The gravitational force depends on liquid density and is not affected by pressure. The pressure gradient depends on the velocities of both phases and on the physical properties of the flowing fluids, as well as the bed geometry characteristics. At atmospheric pressure and low gas velocities, the drag force and pressure gradient are negligible in comparison to the gravitational force. Hence, the flow regime is characterized by a weak gas–liquid interfacial activity and a gravity-driven liquid flow. At elevated pressures, however, higher gas density results from the higher pressure at the given gas and liquid flow rates, which consequently produces a higher drag force at the gas–liquid interphase. At high gas flow, the pressure gradient increases in comparison to the gravitational force, which results in improved liquid spreading over the external particle surface and decreased liquid film thickness. The liquid holdup therefore decreases. The reactor fluid dynamics shift from a state predominantly controlled by gravity to a state controlled by drag force and pressure gradient. Consequently, both elevated pressure and gas flow rate decrease the external liquid holdup. However, as shown in Fig. 4b, the dimensionless variance is independent of the gas pressure at different gas flow rates. Since the dimensionless variance is determined by both the effective diffusion of tracer inside the catalyst pore and the liquid axial dispersion, the experimental observations imply that the former factor is dominant, which is barely affected by the gas flow property.

For different bed porosities, the external liquid holdup increases with increasing liquid flow rate, as is evident in Fig. 5. Higher liquid holdup results from higher resistance, which is comprised of gravity and inertial forces, liquid-side shear stress, and turbulence from local gradients in the velocity field. Increased liquid flow rate enhances the interaction between gas and liquid, which in turn causes turbulences in the liquid film. In addition, liquid-side shear stress increases due to the higher pressure drop of the liquid phase in the bed voidage when more liquid passes through a void space. Consequently, resistance becomes more significant in comparison with the driving force. On the other hand, at a given gas flow rate and pressure, the drag force exerted by the gas side remains constant, which implies that the driving force for the liquid flow does not vary significantly when the liquid flow rate increases. Therefore, the balance between the driving force and resistance becomes favorable for the latter, which leads to higher build up of liquid. For the bed porosity of 0.43, the effects of gas velocity on the external liquid holdup are more considerable at higher liquid flow rates, as shown in Fig. 5, which is in agreement with the findings by Al-Dahhan et al. (1997). However, this is not the case shown for the bed porosity of 0.55, which would be due to

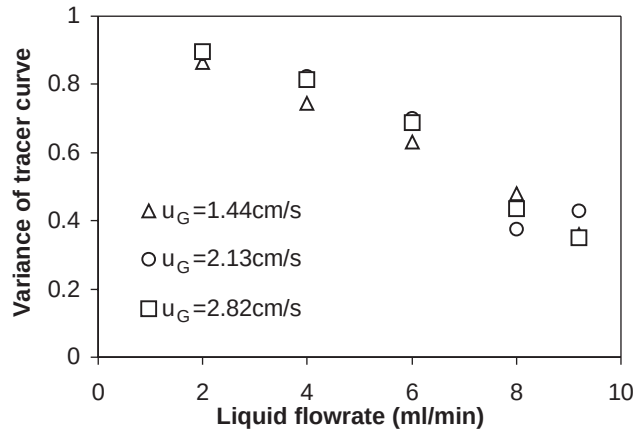

Fig. 6. Effects of liquid and gas flow rate on the dimensionless variances of the tracer curves, bed porosity: 0.55, reactor pressure: 0.8 MPa. (note: 10 ml/min leads to liquid mass flux 0.4 kg/m^2/s).

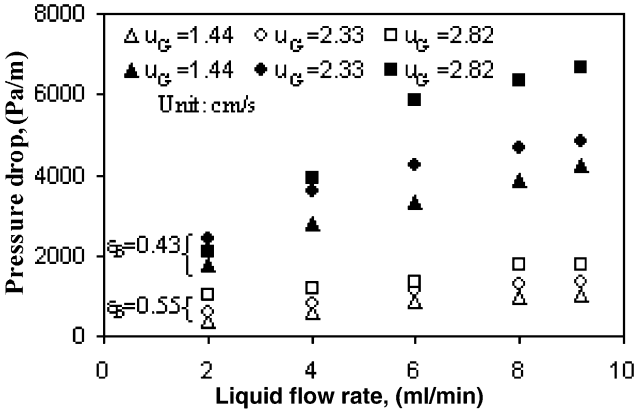

Fig. 7. Effects of liquid and gas flow rate on pressure drop, reactor pressure: 0.8 MPa. (note: 10 ml/min leads to liquid mass flux 0.4 kg/m^2/s).

the truncation error associated with the longer tails of the tracer signal curves.

Fig. 6 exhibits that the dimensionless variance is independent of the gas flow rate, and that it decreases due to the significant reduction of the axial dispersion with an enhancement in liquid flow rate. An increase in the gas or liquid velocity yields higher pressure drop, as shown in Fig. 7. Although liquid holdup decreases at high gas velocity operation due to the decrease of the liquid film thickness, wetting efficiency might increase, which leads to enhanced interaction between gas and liquid phase. Hence, higher pressure drop can be explained by the increased shear stress at the gas–liquid interface. With the decrease in bed porosity, the narrowing free passages in the porous medium experience more pronounced curvatures and more frequent cross-sectional fluctuations, which also result in the elevated pressure drop.

4. Phenomenological model

Holub et al. (1992) developed a phenomenological pore-scale model for two-fluid separated flow in the form of an Ergun-like equation. Valid in the trickle flow regime, this model represents the complex geometry of a porous medium as a simple inclined slit. An outer liquid film fully wets the catalyst wall, and the gas passes through the slit in a plug flow. By neglecting the interfacial gas velocity (slipless) and the gas–liquid interfacial momentum transfer (shearless), this model can handle the conditions under atmospheric pressure. However, at elevated pressure and high gas flow rate, the slipless/shearless model fails to predict the pressure drop, due to the lack of appropriate account for the interfacial interaction between gas and liquid (Al-Dahhan and Dudukovic, 1994). Therefore, Al-Dahhan et al. (1998) extended the Holub model by considering momentum transfer at the gas–liquid interface as a reasonable mechanism for enhancing pressure drop in trickle flow. Two correlations for velocity slip (f_v) and shear slip (f_s) factors were proposed to describe the effect of enhanced interaction on liquid holdup and pressure drop. However, the application of the correlations proposed by Al-Dahhan et al. (1998) in this work was restricted because of several factors. First of all, these correlations were derived for the nonporous solid particles, i.e., glass beads, which exhibit different physical phenomena from the current porous media. Secondly, the discernible dependence of f_v and f_s with respect to Re_L and Re_G was claimed to have a large degree of uncertainty because of the absence of an extensive database. Finally, Ergun's constants, E_1 and E_2, which characterize the bed geometry, have to be determined from the single phase flow experiments and supplied as the input to the extended slit based model before these correlations for f_v and f_s can be used.

On the basis of an extensive trickle flow regime data bank, Iliuta et al. (1998) developed neural network-based correlations for the prediction of shear and velocity slip factors and Ergun single-phase flow bed parameters. The proposed correlations for f_v, f_s and (E_1 and E_2) were fed into Holub's phenomenological slit model and achieved improved predictions of the frictional pressure drops and the external liquid holdups in the trickle flow regime (Iliuta et al., 1998). Therefore, in this work, the extended slit based model aided by generalized neural network correlations is employed to give the theoretical simulation for the porous packing.

The details of the extended Holub model are given in (Al-Dahhan et al., 1998). Only the final form of the governing equations is cited.

$$\psi_G = \frac{\Delta P/L_r}{\rho_G g} + 1 = \left(\frac{\varepsilon_B}{\varepsilon_B - \varepsilon_L}\right)^3 \times \left[\frac{E_1(Re_G - f_v \varepsilon_G Re_i)}{Ga_G} + \frac{E_2(Re_G - f_v \varepsilon_G Re_i)^2}{Ga_G}\right], \quad (5)$$

$$\psi_L = \frac{\Delta P/L_r}{\rho_L g} + 1 = \left(\frac{\varepsilon_B}{\varepsilon_L}\right)^3 \times \left[\frac{E_1 Re_L}{Ga_L} + \frac{E_2 Re_L^2}{Ga_L}\right] + f_s \frac{\varepsilon_G}{\varepsilon_L}\left(1 - \frac{\rho_G}{\rho_L} - \psi_L\right), \quad (6)$$

$$f_v = u_{iG}/u_{iL}, \quad f_s = \tau_{iL}/\tau_{iG}, \quad (7)$$

In fact, the slip factors f_v and f_s in the reactor reflect in an averaged sense the net interaction between gas and liquid in the reactor, because the exact dependence of them on fluid interactions is not deterministic. At any given location in the reactor, different types and levels of interactions are possible, resulting in varying values of f_v and f_s (Al-Dahhan et al., 1998). The original Holub model did not take into consideration the interaction effect, which actually assumes zero values for the slip factors. For the extended model, the slip factors are expected to be functions of a group of flow variables. Given the fluid physical properties and flow rates, the bed and catalyst characteristics, and the operating conditions, the neural network regression enables the prediction of slip factors f_v and f_s, as well as Ergun's constants E_1 and E_2. Then the slit model turns out to be implicit equations with two unknown variables as liquid holdup and pressure drop, which are obtained by solving the equation iteratively using the Newton–Raphson method (Iliuta et al., 2000).

The parity plots for the external liquid holdup (ε_e) and pressure drop ($\Delta P/H$) are shown in Figs. 8a and b. The average absolute relative errors (AARE) for the liquid holdup and pressure drop are 16.2% and 28.3%, respectively. Therefore, the extended slit based model predicts reasonably the effect of the gas and liquid flow rates, the reactor pressure, and the bed characteristics. However, it is noteworthy that the employed model always underpredicts the value of (ε_e) and ($\Delta P/H$). The occurrence of diffusion of tracer in the particles resulted in a long tail on the tracer curve. The major disadvantage of the moments approach is that the tail of the tracer curve plays a strong role. Even though the mass balance of tracer was shown to be conserved, the long tail makes the cutoff of the tracer curve not easily determinable, and consequently the physical characteristics of the liquid phase are distorted. This might lead to errors in the calculation of the first moment. Therefore, the value of residence time could be amplified, which leads to the higher values of experimental observations on external liquid holdup.

The total pressure gradient is comprised of frictional, gravitational, and acceleration/deceleration components, where the effects of the acceleration/deceleration term were always assumed to be marginal for the trickle flow measurement. The frictional pressure gradients for the porous particle could be more significant than for the nonporous particle because of the capillary phenomena inside the particle pore. Therefore, the effect of friction pressure in the porous media could be underpredicted, since the model is originally designed for nonporous particles. In addition, we are using correlations proposed by neural network regression in this work. Even though the database employed to derive such correlations is elaborate, the majority of them are based on glass beads and other nonporous materials (Iliuta et al., 1998). It is possible that the reliability of the derived correlation for porous particles is not as good as for nonporous particles. Hence, more data collection using porous media is recommended to understand and quantify the effect of intraparticle diffusion.

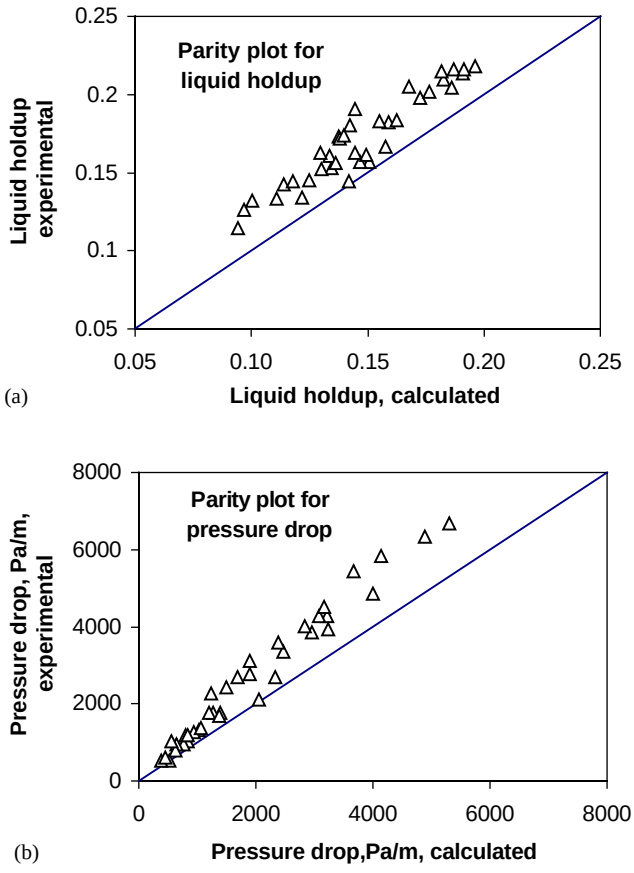

Fig. 8. Parity plot for (a) liquid holdup and (b) pressure drop by comparing the experimental observations with the theoretical calculation from extended Holub model.

5. Conclusion

For a trickle-bed reactor with porous particles, intraparticle diffusion of the tracer plays a key role in the estimation of liquid holdup. The dimensionless variance is independent of the reactor pressure and gas flow rate based on the conditions used in this study, even though the external liquid holdup is affected by them. The increase of liquid flow rate weakens the dimensionless variance, but enhances the external liquid holdup and pressure drop. The extended slit based model was employed for the prediction of the frictional two-phase pressure drop and the liquid holdup, where shear and velocity slip factors are necessary for the improved predictions. The correlations used for the calculation of slip factors

and bed Ergun constants rely on artificial neural networks, dimensional analysis, and a large trickle-flow database. The combination of the extended slit based model and the neural network correlation allowed achieving predictions for the liquid holdup and pressure drop with AARE of 16.2% and 28.3%, respectively. More data at elevated pressure for porous catalyst are necessary for improved neural network based correlations to give more accurate predictions.

Notation

AARE	average absolute relative error, AARE $= \sum_{i=1}^{N} \lvert(y_{\mathrm{Sim}\,i} - y_{\mathrm{Exp},i})/y_{\mathrm{Exp},i}\rvert/N$
C	Concentration of tracer in flowing stream, mg/ml
E_1, E_2	Ergun equation constants for single phase flow
Ga_α	Galileo number of α phase, $Ga_\alpha = (g d_p^3 \varepsilon_B^3/\nu_\alpha^2(1-\varepsilon_B)^2)$
L_r	bed height, m
Re_i	interfacial Reynolds number
Re_α	Reynolds number of α phase, $(u_\alpha d_p/\nu_\alpha(1-\varepsilon_B))$
u_α	superficial velocity of α phase, m/s

Greek letters

ε_e	external liquid holdup
ε_i	internal liquid holdup
$\varepsilon_{l,t}$	total liquid holdup
μ	mean of response
σ_θ^2	dimensionless variance of tracer curve
σ^2	dimensional variance of tracer curve
τ	liquid residence time in packed bed
ψ_α	dimensionless pressure drop of α phase

Subscript

α	general subscript meaning gas (G) or liquid (L) phase

Acknowledgements

The financial supporters of the Chemical Reaction Engineering Lab (CREL) are gratefully acknowledged.

References

Al-Dahhan, M.H., Dudukovic, M.P., 1994. Pressure drop and liquid holdup in high-pressure trickle-bed reactors. Chemical Engineering Science 49, 5681.

Al-Dahhan, M.H., Larachi, F., Dudukovic, M.P., Laurent, A., 1997. High-pressure trickle-bed reactors: a review. Industrial and Engineering Chemistry Research 36, 3292.

Al-Dahhan, M.H., Khadilkar, M.R., Wu, Y., Dudukovic, M.P., 1998. Prediction of pressure drop and liquid holdup in high-pressure trickle-bed reactors. Industrial and Engineering Chemistry Research 37, 793.

Fortuny, A., Ferrer, C., Bengoa, C., Font, J., Fabregat, A., 1995. Catalytic removal of phenol from aqueous phase using oxygen or air as oxidant. Catalysis Today 24, 79.

Gupta, P., Al-Dahhan, M.H., Dudukovic, M.P., Mills, P.L., 1999. Novel signal filtering methodology for obtaining liquid phase tracer responses from conductivity probes. Flow Measurement Instrumentation 11, 2.

Holub, R.A., Dudukovic, M.P., Ramachandran, P.A., 1992. A phenomenological model of pressure drop, liquid holdup and flow regime transition in gas–liquid trickle flow. Chemical Engineering Science 47, 2343.

Iliuta, I., Thyrion, F.C., Muntean, O., Giot, M., 1996. Residence time distribution of the liquid in gas–liquid cocurrent upflow fixed-bed reactors. Chemical Engineering Science 51, 4579.

Iliuta, I., Larachi, F., Grandjean, B.P.A., 1998. Pressure drop and liquid holdup in trickle flow reactors: improved ergun constants and slip correlations for the slit model. Industrial and Engineering Chemistry Research 37, 4542.

Iliuta, I., Larachi, F., Al-Dahhan, M.H., 2000. Double-slit model for partially wetted trickle flow hydrodynamics. A.I.Ch.E. Journal 46, 597.

Levec, J., Saez, A.E., Carbonell, R.G., 1986. Hydrodynamics of trickling flow in packed beds. A.I.Ch.E. Journal 32, 369.

Sater, V.E., Levenspiel, O., 1966. Two-phase flow in packed beds: evaluation of axial dispersion and holdup by moment analysis. Industrial and Engineering Chemistry Fundamentals 5, 86.